

AD-R164 312

THE INFLUENCE OF MICROSTRUCTURE ON THE STRENGTH AND  
TOUGHNESS AND THE FAT. (U) FOREIGN TECHNOLOGY DIV  
WRIGHT-PATTERSON AFB OH L HUANG ET AL. 24 JAN 86

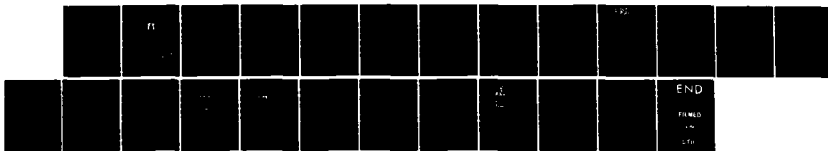
1/1

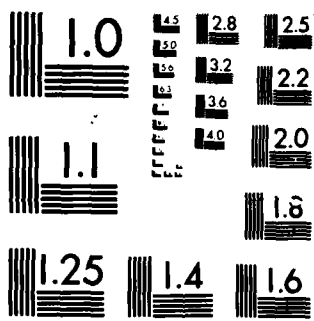
UNCLASSIFIED

FTD-ID(R5)T-1156-85

F/G 11/6

NL





MICROCOPY RESOLUTION TEST CHART  
NATIONAL BUREAU OF STANDARDS 1961 A

FTD-ID(RS)T-1156-85

AD-A164 312

## FOREIGN TECHNOLOGY DIVISION

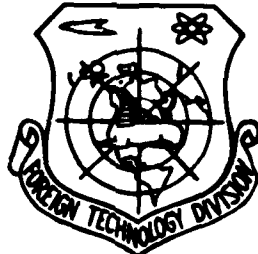


THE INFLUENCE OF MICROSTRUCTURE ON THE STRENGTH AND TOUGHNESS AND  
THE FATIGUE CRACK PROPAGATION IN CrWMn STEELS

by

Litong Huang and Yunbo Chen

DTIC FILE COPY



S DTIC  
ELECTED  
FEB 19 1986  
A

Approved for public release;  
distribution unlimited.



86 2 10 246

FTD -ID(RS)T-1156-85

## EDITED TRANSLATION

FTD-ID(RS)T-1156-85

24 Jan 86

MICROFICHE NR: FTD-86-C-001415

THE INFLUENCE OF MICROSTRUCTURE ON THE STRENGTH AND  
TOUGHNESS AND THE FATIGUE CRACK PROPAGATION IN CrWMn  
STEELS

By: Litong Huang and Yunbo Chen

English pages: 20

Source: Jin Shu Re Chu Li, Nr. 2, 1984, pp. 22-30

Country of origin: China

Translated by: SCITRAN

F33657-84-D-0165

Requester: FTD/TQTA

Approved for public release; distribution unlimited.

A1

THIS TRANSLATION IS A RENDITION OF THE ORIGINAL FOREIGN TEXT WITHOUT ANY ANALYTICAL OR EDITORIAL COMMENT. STATEMENTS OR THEORIES ADVOCATED OR IMPLIED ARE THOSE OF THE SOURCE AND DO NOT NECESSARILY REFLECT THE POSITION OR OPINION OF THE FOREIGN TECHNOLOGY DIVISION.

PREPARED BY:

TRANSLATION DIVISION  
FOREIGN TECHNOLOGY DIVISION  
WPAFB, OHIO.



FTD-ID(RS)T-1156-85

Date 24 Jan 1986

**GRAPHICS DISCLAIMER**

All figures, graphics, tables, equations, etc. merged into this translation were extracted from the best quality copy available.

THE INFLUENCE OF MICROSTRUCTURE ON THE STRENGTH AND TOUGHNESS  
AND THE FATIGUE CRACK PROPAGATION IN CrWMn STEELS

Litong Huang and Yunbo Chen\*

Peking Institute of Electrical Engineering,  
Industry Dept. of Mechanical Engineering

ABSTRACT

In this paper, we describe the interrelation between the microstructures of CrWMn high carbon steels of cold punch dies and strength, fracture resistance at static bending state, deflection and fracture toughness after various heat treatments. The influence of microstructures on the pregnant period of the fatigue crack No and the fatigue crack growth rate  $da/dN$  is also studied. Our experimental results show that after carbides refining pretreatment, the quenching and tempering structures have maximum strength, the No increases remarkably and the  $da/dN$  decreases at the low stress intensity factor  $\Delta K$  range. After carbides refining pretreatment, the isothermal quenching structures have the best combination of strength and toughness if a mixed martensite structure with 50% bainite is obtained. It also can prolong the pregnant period of nucleation of fatigue cracks and reduce  $da/dN$  at the midstream intensity factor  $\Delta K$  range.

According to the examination of fatigue fractures by a scattering electron microscope, the fracture of a conventional quenching and tempering structure with coarse carbides is mainly intergranular. It has low No and high  $da/dN$ . On the other hand, for an isothermal quenching structure after carbides refining pretreatment, its percentage of dimples in the fracture increases. It

---

\*Chinsen Chang and Faikung Zhu also participated in this experiment.

has high  $N_0$  and low  $da/dN$ . If the bainite is more than 90%, its fracture will show the characteristic of quasicleavage and  $da/dN$  increases remarkably. Therefore, it is obvious that  $N_0$  and  $da/dN$  are closely related to the microfracture mechanism.

## 1. Introduction

High carbon low alloy steels have been used frequently in the parts of bearings, rollers and cold punch dies. During operation, they usually will fail because of fatigue fracture and brittle fracture at the early stage. In order to best utilize metal materials, different heat treating techniques should be employed for different purposes of application. And the steel structure should be controlled by adjusting various operational parameters such that the best combination of strength and toughness can be obtained. Finally, stress should be tolerated and the resistance to micro-cracks and crack propagation should be increased. These are very important for high carbon high strength steel in order to prevent brittle fracture at an early stage and to prolong the fatigue life time of the parts of various tools.

In the last decade a lot of research has been done to improve the properties of high carbon steels. C. A. Stikels [1] first proposed the techniques of carbide refining and ultrafining for bearing steel. The influence of carbide refining on the properties of high carbon steel was further described in [2-4]. Experiments showed that carbide refining could increase the hardness, the contact fatigue resistance and the wear resistance of steels remarkably. However, it had a bad effect on fracture toughness, impact toughness and ductility. Since high carbon cold punch dies and moving and loading parts usually sustain larger impact loading and are operated under high stress, how to increase strength and toughness simultaneously is an urgent problem needing to be solved.

Recently, from the studies of mixed structures of bainite and martensite, it was discovered that if a sufficient amount of

bainite is added to the high strength martensite matrix, this structure not only has high strength, but its ductility and fracture toughness also increase remarkably [5-7]. However, the effect of the microstructure on the strength and toughness and the formation and propagation of fatigue cracks is still seldom studied. The study of those materials with high carbon, high strength and high brittleness is even less promising due to the difficulty of manufacturing and assembling these materials.

In this paper we use high carbon CrWMn steel as material. By employing different techniques of heat treatment, various sizes and distributions of carbide grains as well as various percentages of bainite on the martensite matrix can be obtained. Based on these, we will study the effect of the microstructure on the strength and toughness, the initiation of fatigue cracks, and the growth rate of fatigue cracks.

## II. Techniques of heat treatment and experimental methods

The chemical composition of our high carbon CrWMn steel is: 0.93% C, 0.62 % Cr, 0.78% W and 1.17% Mn. The initial structure after pretreating by conventional spheroidization and solid-dissolve-refining spheroidization, is quenched, tempered and then isothermally quenched with various time durations. The heat treating techniques and microstructure are listed in Table 1. Except for conventional spheroidization, all the specimens are heat treated in the medium and high temperature furnace.

The specimens are tensed by  $\phi$  6x80 mm collet. By using a tension meter and from the measured tensile curve,  $\sigma_b$  and  $\sigma_{0.2}$  can be obtained. The fracture load of the notch at static bending state  $P_b$  and the deflection  $f$  can be obtained from the loading-deflection curve which is determined by static bending experiments. The dimension of the specimen above is 10x10 mm with thickness of 50 mm, and the radius of notch  $r$  is 0.1 mm. The fracture toughness is determined from the 10x20x100 mm specimen with a three points

bend, and the data are the average of three specimens. The formation and propagation of fatigue cracks are investigated on the 10x10x60 mm specimen with a notch (radius of notch is 0.1 mm). All the experiments above are done by an Instron-1255 testing machine under static and dynamic states.

The dimensions of carbide and the bainite after special etching are examined by a QT-720 photographic analyzer. The fracture facet of the specimen with fracture toughness and the fracture facet of the specimen with growing fatigue cracks are inspected by an X-650 scattering electron microscope (SEM). Their fracture morphologies are taken under various ranges of stress intensity factor K.

Table 1. Heat treating techniques and structure

Technique index No.	Pretreatment		Final heat treatment	
	Technique	Structure	Technique	Structure
I <sub>a</sub>	Spheroidize annealed 820°C x 2h → 700°C x 5h	Coarse carbides 0.9-1.5um	860°C oil quenched, 250°C tempering	Tempering martensite
I <sub>b</sub>			860°C, 260°C isothermal 1 h	50% bainite + martensite
II <sub>a</sub>	solid-dissolve-refining spheroidization	fine carbides uniform distribution 0.5 ~0.7 um	860°C, 260°C isothermal 20 min.	20% bainite + martensite
II <sub>b</sub>	1050°Cx0.5 h, 300°C isothermal		860°C, 260°C isothermal 1 h	50% bainite + martensite
II <sub>c</sub>	0.5h, 800°C x1h air cool → 700°C x 4 h		860°C, 260°C isothermal 3 h	90% bainite + martensite
II <sub>d</sub>			860°C oil quenched, 250°C tempering	tempering martensite

### III. Experimental results and analysis

#### 1. Microstructure

Figures 1a-1f are the metallographs of the specimen after various heat treatments. The initial structure of high carbon CrWMn steel pretreated by conventional spheroidized annealing has carbide about 0.9-1.5  $\mu\text{m}$  after 860°C quenching (see Figures 1a-1b). If it is pretreated by solid-dissolve-refining spheroidization and later treated by 860°C quenching, then it has uniformly distributed carbides with size of 0.6  $\mu\text{m}$  as shown in Figure 1f.

Figures 1c-1e are the metallographs of specimens which are pretreated by refining spheroidization and then isothermal quenching under different time durations and having different percentages of bainite. When the percentage of bainite is less than 29%, needle-like shapes will show up individually on the surface as shown in Figure 1c. When bainite is 50%, its structure has a bush-like distribution (see Figure 1d). If the isothermal time increases to 3 h, the bainite will increase to 90% (see Figure 1e).

#### 2. Experimental results and analysis of mechanical properties

The testing data of tension and static bending are listed in Table 2 and shown in Figures 2 and 3.

As shown in Table 2, the structure of refining spheroidization and low temperature tempering has maximum strength (technique IIId). Its  $\sigma_b$  is 25% more than that of technique Ia, but its ductility (bending resistance, deflection, etc.) and fracture toughness  $K_{Ic}$  remain the same. This is consistent with W. C. Luty's result of 52100 bearing steel and our results of GCrl5 steel and rolled steel [2,4,7].

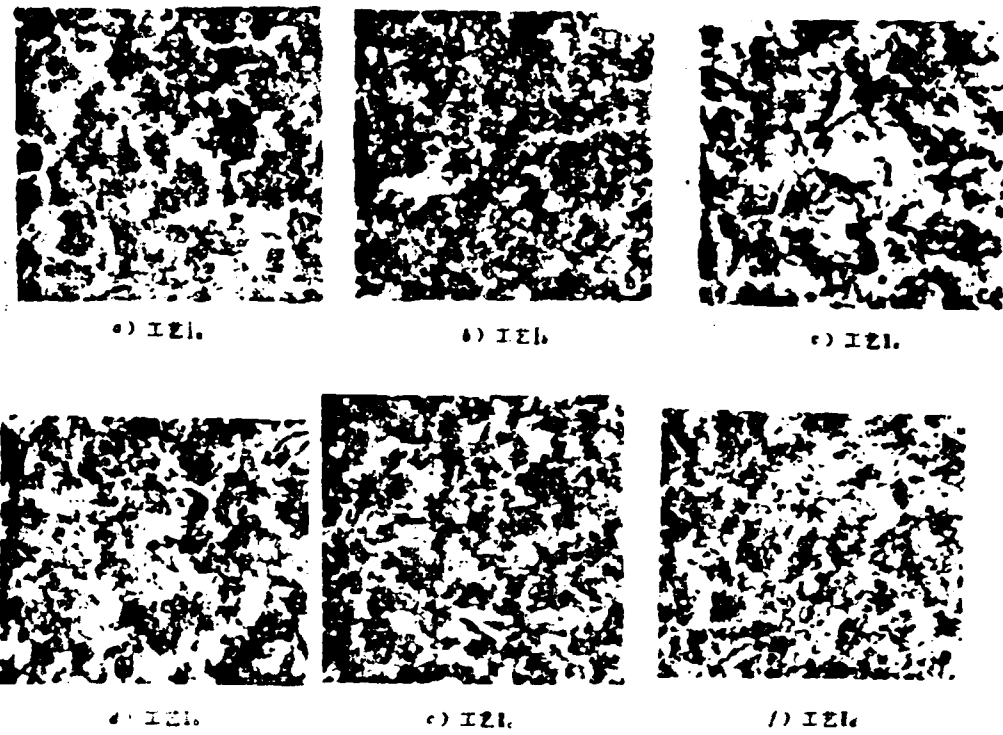


Fig. 1 Microstructures obtained by various techniques of heat treatment  $\times 800$ . a) technique Ia, b) technique Ib, c) technique IIa, d) technique IIb, e) technique IIc, f) technique IId.

Table 2 Mechanical properties of structures under various heat treatments

Technique index No.	Hardness (HRC)	Ultimate strength (Kgf/mm <sup>2</sup> )	Ultimate yield (Kgf/mm <sup>2</sup> )	Fracture load at static bending state (Kgf)	Reflection f (mm)	Fracture toughness $K_{Ic}$ (Kgf/mm <sup>3/2</sup> )
I <sub>a</sub>	60.5	192.6	159.8	645	0.165	62.5
I <sub>b</sub>	67.0	206.2	160.5	680	0.172	67.3
II <sub>a</sub>	61.5	211.5	188.9	691	0.182	63.6
II <sub>b</sub>	61.5	219.6	198.57	710	0.192	74.2
II <sub>c</sub>	55.5	213.1	185.2	680	0.187	62.1
II <sub>d</sub>	61.5	236	218.7	643	0.165	63.9

Figure 2 shows the relation between the percentage of bainite and the hardness as well as the strength after the treatments of refining spheroidization and isothermal quenching with different time durations. As shown in Figure 2, the strength of martensite ( $M$ ) decreases with increasing percentage of bainite ( $B$ ). This is because  $M$  and  $B$  have different strength in their mixed structure. During transformation there exists an inhomogeneous strain such that the strength of the mixed structure is lower than that predicted by the mixing rule [6]. For high strength material, however, if a sufficient amount of bainite (in this paper it is 50% for high carbon CrWMn steel) is added to the martensite matrix, its fracture loading at static bending state  $P_b$ , deflection  $f$  and fracture toughness  $K_{lc}$  will reach maximum values. This structure thus has a better combination of strength and toughness (see Figure 3).

### 3. The influence of microstructure, strength and toughness on the formation and propagation of fatigue cracks.

To have better fatigue strength, the bulk material without cracks at the initial condition is usually used. The fatigue fracture can be determined from the strength. The higher the strength, the higher the ultimate fatigue. In fact, there always exist some defects, impurities and microfractures inside the tool parts. The microstructures of high strength and high brittleness materials obviously have some effects on their strength and toughness, and the formation and propagation of fatigue cracks.

The fracture of materials (including fatigue fracture) has three stages: birth of cracks, crack propagation and fracture. According to experiments, the crack's pregnant period  $N_o$  not only depends on the stress condition and stress level, but also strongly depends on the material's microstructure and properties. The growth rate  $da/dN$  of fatigue cracks is high for high strength materials.  $N_o$  has the largest percentage in total fatigue life  $N_f$ . It is thus very important to study the effect of the microstructure and the strength and toughness of high carbon high strength materials on  $N_o$ .

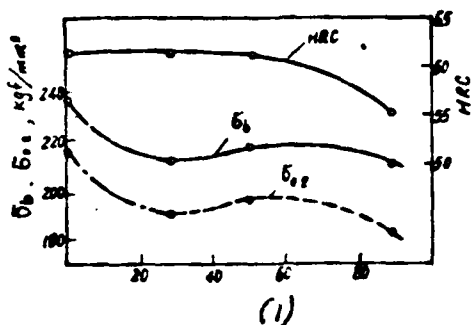


Fig. 2 The percentage of bainite vs strength and toughness.  
 (treated by carbide refining techniques II<sub>a</sub>, II<sub>b</sub>, II<sub>c</sub>,  
 and II<sub>d</sub>) (1: percentage of bainite)

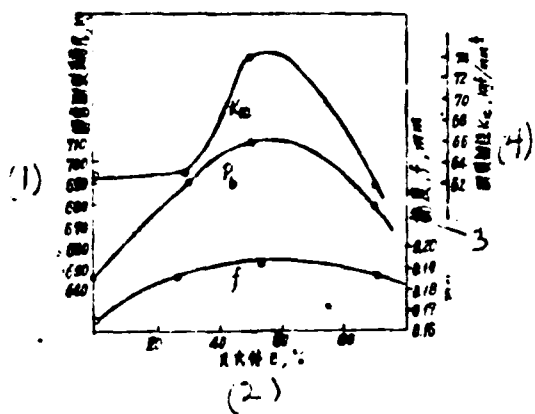


Fig. 3 The percentage of bainite vs fracture toughness  $K_{lc}$ , fracture  
 load at static bending state  $P_0$ , and deflection  $f$ .  
 (treated by carbide refining techniques II<sub>a</sub>, II<sub>b</sub>, II<sub>c</sub>, and  
 II<sub>d</sub>) (1: fracture load at static bending state; 2: percentage;  
 3: deflection; 4: fracture toughness)

(1) Pregnant period  $N_o$  of fatigue cracks: The stress cycle period of fatigue cracks before a 0.1-0.2 mm crack appears is called either the conditional life without crack No. 1 or the pregnant period of the crack's birth  $N_{0.20}$  depending on different testing machines and methods. The  $N_o$  values of various heat treating structures are listed in Table 3.

It is shown in Table 3 that: (1) the  $N_o$  value of quenching, tempering or isothermal quenching structures pretreated by refining spheroidization is much higher than that pretreated by conventional spheroidization. Carbide refining and uniform distribution of carbides can increase the fatigue crack's pregnant period  $N_o$  remarkably. (2)  $N_o$  is controlled by the microstructure and the strength and toughness of materials. The quenching and tempering structure (technique IIId) with fine carbides, which has the highest strength, and the martensite structure mixed with 50% bainite (pretreated by carbide refining and treated by isothermal quenching, technique IIB), which has the best combination of strength and toughness, have the highest  $N_o$  values. (3) The  $N_o$  value of the quenching and tempering structure pretreated by conventional spheroidization is comparable to the  $N_o$  value of the isothermal quenching structure pretreated by conventional spheroidization. This implies that when the carbide grain is coarse and not uniformly distributed, bainite has little effect on  $N_o$ .

(2) Growth rate  $da/dN$  of fatigue cracks: fracture mechanics is employed to study the influence of microstructure on the fatigue crack propagation under various heat treatments. By using a computer, the measured crack propagating length  $a$  and its corresponding cycling number  $N$  can be fitted into a formula by the least square method. The formula of Paris  $da/dN = c (\Delta K)^m$  is used here and also plotted in the figure.

Figure 4 is the  $da/dN - \Delta K$  curves under various heat treatments. After the carbide refining treatment, the fatigue threshold value  $\Delta K_{th}$  and the crack growth rate  $da/dN$  of high carbon steel can be reduced remarkably.

Table 3. The pregnant period  $N_o^*$  of fatigue cracks of various heat treating structures

Technique index No.	Technique of heat treatment	Microstructure	First observe crack's length (mm)	Pregnant period of crack $N_o \times 10$
I <sub>a</sub>	conventional spheroidization 860°C quenching, 250°C tempering	Tempering martensite structure with coarse carbides	0.17	7.7
I <sub>b</sub>	conventional spheroidization 860°C isothermal quenching 1 h	Martensite structure with 50% bainite and coarse carbides	0.21	8.5
II <sub>a</sub>	Refining spheroidization 860°C isothermal quenching 20 min	Martensite structure with 29% bainite and fine carbides	0.18	19.0
II <sub>b</sub>	Refining spheroidization 860°C isothermal quenching 1 h	Martensite structure with 50% bainite and fine carbides	0.20	37.5
II <sub>c</sub>	Refining spheroidization 860°C isothermal quenching 3 h	Martensite structure with 90% bainite and fine carbides	0.17	30.0
II <sub>d</sub>	Refining spheroidization 860°C quenching 250°C tempering	Tempering martensite structure with fine carbides	0.23	38.0

\* Loading system is  $P_{max} / P_{min} = 330 \text{ Kg} / 150 \text{ Kg}$

Figure 5 shows the crack's growth rate at various  $\Delta K$  vs. the percentage of bainite after the carbide refining treatment. As shown in the figure, at low stress intensity factor  $\Delta K$  range ( $\Delta K = 36 \text{ Kgf/mm}^{3/2}$ ) which is close to threshold value, the growth rate of fatigue cracks is low for those carbide refined quenching and tempering structures which have the highest strength. This is consistent with the observation of their high  $N_0$  value (see Table 3).  $da/dN$  increases sharply with increasing  $\Delta K$  due to higher  $m$  value. When  $\Delta K > 40 \text{ Kgf/mm}^{3/2}$ , the mixed structure with 50% of bainite has the minimum value of  $da/dN$ . This is related to the increase of fracture toughness and ductility.

#### 4. Effect of microstructure on the fracture morphology of fatigue specimens

The fracture surface of a fatigue specimen is placed perpendicular to the optical axis of the SEM and is examined continuously along the propagating direction of its crack. Figure 6 shows the morphology of the initial area of a fatigue crack around the crack notch. Under the effect of stress, the initial propagating crack of the fatigue crack has some certain angle with respect to the fracture surface. For the quenching and isothermal quenching structure pretreated by conventional spheroidization, the crack path at the root of the crack notch has cleavage facets and is transgranular as shown in Figure 6a. For the fracture of those carbide refining quenching, tempering and isothermal quenching structures, cleavage and transgranular fracture are reduced remarkably. The fracture mechanism is mainly of microvoid coalescence (see Figures 6b-6c). For the M/B mixed structure, some twisted strips consisting of small dimples show up at the crack's propagating path and at the top of the specimen (see Figure 6d).

Figure 7 shows the fracture morphology of the fatigue crack propagation under a medium stress intensity factor range,  $\Delta K = 40 - 50 \text{ Kgf/mm}^{3/2}$ . For the quenching and tempering structure with

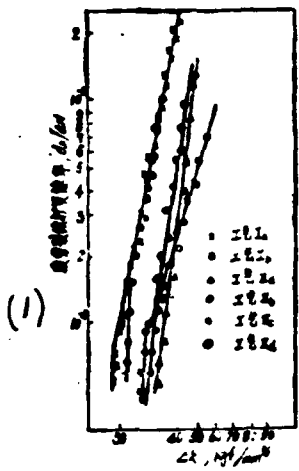


Fig.4 The  $da/dN$  -  $\Delta K$  curves of various heat treating techniques.  
( 1: growth rate of fatigue cracks)

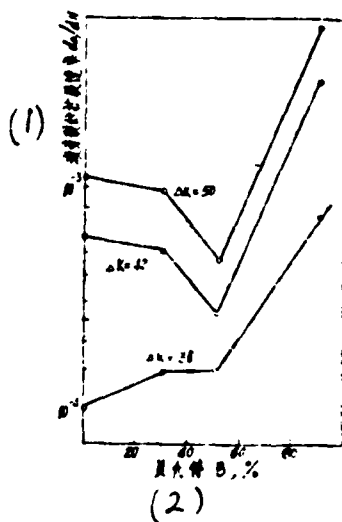


Fig.5 The percentage of bainite vs the growth rate of fatigue cracks at various  $\Delta K$ .  
( 1: growth rate of fatigue cracks; 2: percentage of bainite)

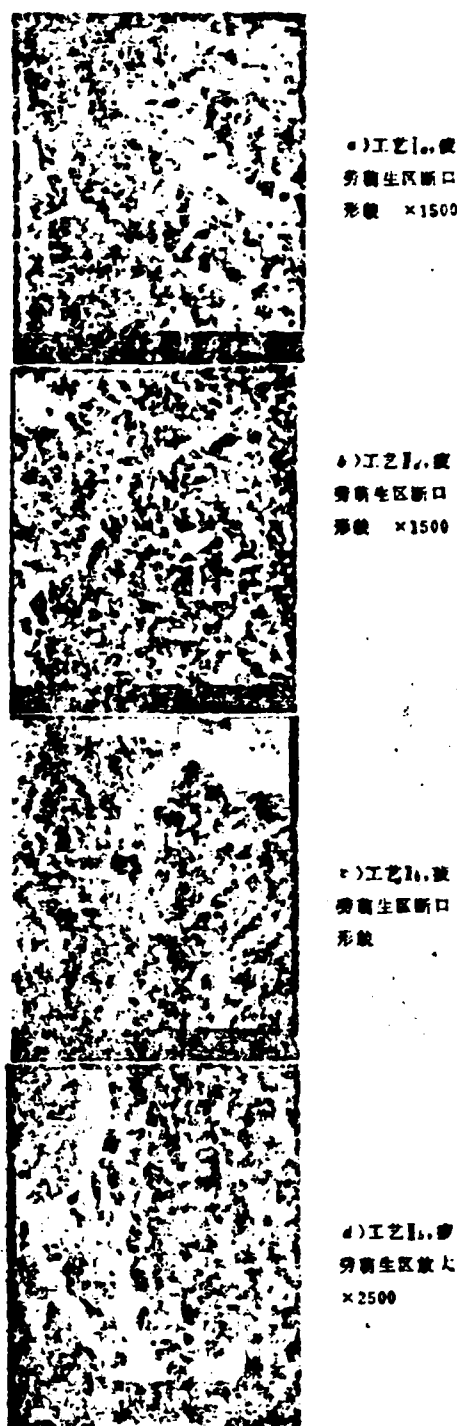


Fig.6 The SEM morphology of fracture surface at the area of initial fatigue crack around the crack notch for various heat treating structures ( $\Delta K = 36 \text{ Kgf/mm}^{3/2}$ ). (The white strip which has some angle with respect to fracture is the initial fatigue crack) (a) Technique index I, fracture morphology at the area of initial fatigue crack,  $\times 1500$ ; (b) Technique II<sub>c</sub>, morphology at the area of initial fatigue crack,  $\times 1500$ ; (c) Technique II<sub>d</sub>, morphology at the area of initial fatigue crack; (d) Technique II<sub>b</sub>, morphology at the area of initial fatigue crack,  $\times 2500$ .

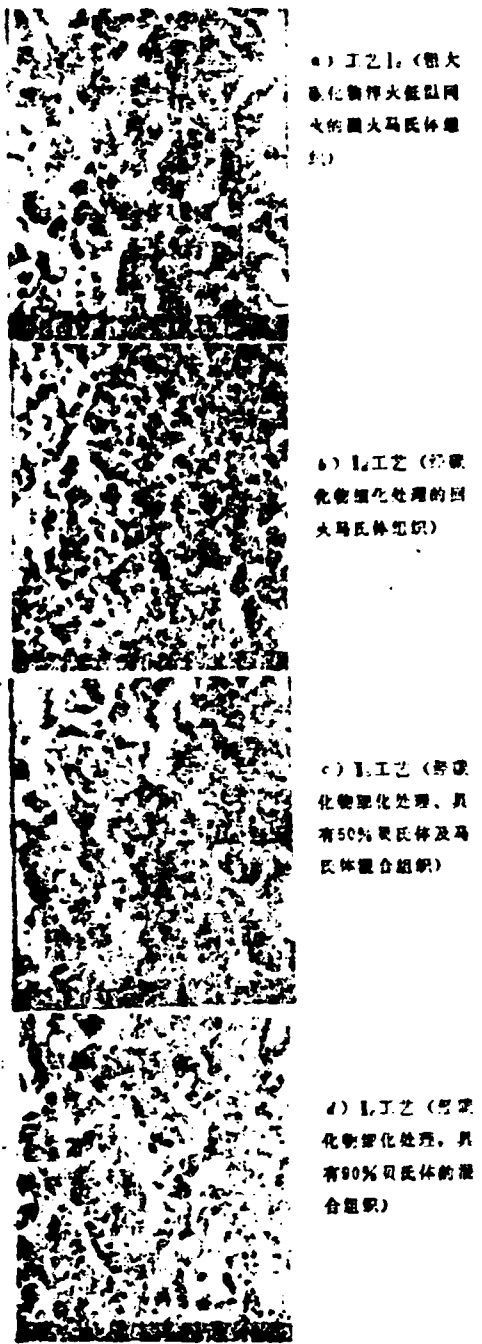


Fig.7 The fracture morphology of growing fatigue at  $4K=40\sim 50 \text{ Kg/mm}^2$  after various heat treatments. (a) Technique I (tempering martensite structure treated by coarse carbide quenching and low temperature tempering); (b) Technique II<sub>a</sub> (tempering martensite structure treated by carbide refining); (c) Technique II<sub>b</sub> (martensite structure mixed with 50% bainite and treated by carbide refining); (d) Technique II<sub>c</sub> (mixed structure with 90% bainite and treated by carbide refining).

conventional spheroidization, its fracture facet is mainly intergranular and has a small amount of dimples as shown in Figure 7a. For the quenching and tempering structure with carbide refining, its fracture facet has small dimples and small cleavage facets (see Figure 7b). For the mixed structure with 50% of bainite, its fracture facet has the highest percentage of dimples (see Figure 7c). This is consistent with the observation that it has a low crack growth rate. When the percentage of bainite increases to 90%, its fracture facet changes from the mixture of small dimples and quasicleavage to quasicleavage facets as shown in Figure 7d. In this case, a high crack growth rate will appear again as shown in Figures 4 and 5. This microfracture mechanism can be used to explain why the CrWMn steel in [8] after isothermal quenching time exceeding 1 h ( $B > 50\%$ ), has lower toughness and ductility and a much shorter life time.

#### IV. Discussion

##### 1. The effect of carbide of high carbon steel on strength and toughness, and pregnant period of fatigue crack No:

The carbide in high carbon steel remains in the steel as a brittle second phase and becomes the nucleation of cleavage fractures. On the other hand, the size and number of carbides have direct effect on the movement of dislocation, and thus increase the material's ductile resistance and then its strength. During the carbide refining process in high carbon steel, the austenite also can be refined such that the strength and toughness of the steel can be enhanced. Therefore, the effect of carbide on the strength and toughness of high carbon steel is very complicated.

The coarse carbide ( $D > 1 \mu\text{m}$ ) in high carbon steel usually is the origin of cracks [9]. Especially when the carbides distribute along the crystal boundary, the material will have strong brittleness. For high carbon CrWMn steel heat treated by conventional spheroidized quenching, its carbides tend to have network

distribution and larger grain size [8]. The fatigue fracture facet is mainly transgranular and the fracture mechanism is due to microvoid coalescence as shown in Figure 7a. From the Auger energy spectrum, Krauss, et al., showed that the transgranular fracture in high carbon steel is caused by the clusters of carbon and phosphorus existing along the crystal boundary. The bigger the grain size, the easier the transgranular fracture [10]. After the quenching, tempering or isothermal quenching structure pre-treated by conventional spheroidization is etched by heavy potassium sulphuric acid and is examined by SEM, the carbide impurities are found distributed along the crystal boundary as shown in Figure 8a. This is consistent with the SEM observation that the fatigue fracture is mainly transgranular (see Figure 7a).

Under transformation stress, the coarse carbide on the surface will separate from the base body and cause the formation of fatigue cracks. The bigger the carbide, the more intense the stress. The separation from the base body and the formation of cracks are thus easier [9] and the pregnant period of fatigue cracks becomes shorter. The carbide second phase structure has larger grain size and has carbide clusters along the crystal boundary. After the crack is formed, the crack under transformation stress will propagate rapidly along the path of the crystal boundary which has lowest energy consumption. In this case, the crack growth rate  $da/dN$  is high as shown in techniques  $I_a$  and  $I_b$  of Figure 4.

The quenching and tempering structure with refining spheroidization has a uniform distribution of carbide instead of a network distribution as shown in Figure 8b. The crystal grain can be refined to the 11th degree as shown in Figure 9. Both the carbide refining and crystal grain refining can enhance its strength remarkably. However, its fracture toughness and ductility are almost the same as those of quenching and tempering structures with conventional spheroidization. This is because the mean carbide spacing decreases with increasing the carbide refining and its number. In other words, the ductile, transformable area before a

fracture occurs will decrease such that ductility is reduced. This will cancel out the increase of ductility caused by crystal grain refining. The carbide refining structure by quenching and tempering is mainly used for improving its strength. This can thus be used to increase contact fatigue and wear resistance [2]. Carbide refining can remarkably reduce the number of large grains which is the origin of cracks. This will make the yield strength stronger, ductile transformation more difficult and cracks harder to be formed [11]. The pregnant period  $N_0$  of fatigue cracks thus becomes longer, and the ratio of life time without cracks to total life time will increase.

## 2. The strength and toughness and fatigue properties of martensite and bainite mixed structures

Since cracks propagate mainly inside the base body, the mechanical parameters and structure characteristics of the base body will strongly affect the propagating path of cracks and the fracture mechanism. From the inspection of fatigue fracture facets, the number of dimples in the fracture facet of an isothermal quenching structure pretreated by conventional spheroidization is higher than that of a quenching and tempering structure. For an M/B mixed structure pretreated by refining spheroidization, its intergranular fracture is reduced largely and the number of dimples increases remarkably. When the percentage of bainite reaches 50%, intergranular fractures almost disappear. A microvoid can be easily seen on the crack tip in this M/B mixed structure as shown in Figure 6c-d. Since the bainite structure has better ductility, it can relieve the three-way stress on the fatigue tip effectively through ductile transformation. Therefore, it can shift the fracture mechanism from intergranular brittle fracture to microvoid fracture. This will reduce the crack growth rate remarkably (see Figure 4, Techniques II<sub>a</sub> and II<sub>b</sub>). The experimental results also show that a 50% bainite structure has the minimum value of  $da/dN$  as  $\Delta K$  is increasing (see Figure 5). But if bainite increases to 90%, fracture facets will show the characteristic of quasicleavage

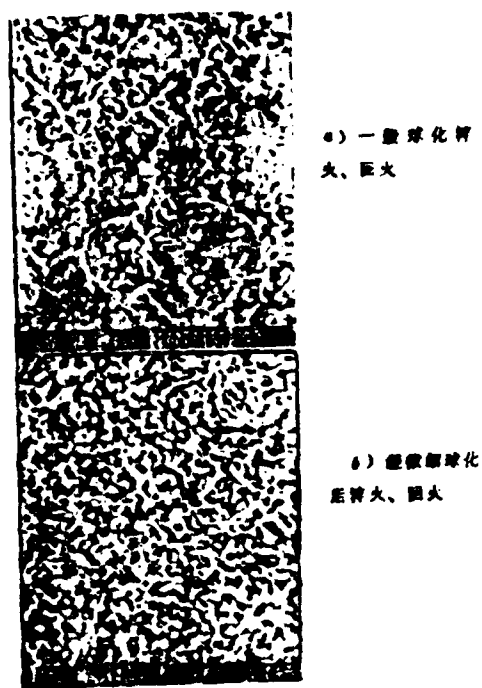


Fig. 8 The carbide second phase grain distribution in the quenching and tempering structure after conventional spheroidization and refining spheroidization (SEM x2000). (a) conventional spheroidized quenching and tempering; (b) quenching and tempering after refining spheroidization.

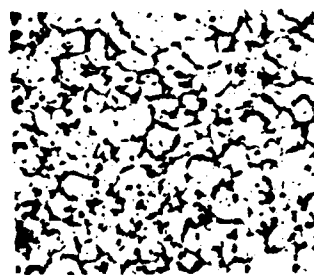


Fig. 9 The 11<sup>th</sup> degree crystal grains after refining spheroidized quenching and tempering. x 500.

(see Figure 7d). In this case, the ductility and fracture toughness decrease, and the crack growth rate  $da/dN$  increases to the level of conventional spheroidized structures (see Figure 4 technique II<sub>C</sub>).

If the M/B mixed structure has the proper combination during isothermal quenching, the initial bainite will cut off those austenite grains such that the size of martensite which is formed later becomes smaller. The fracture element decreases markedly compared to the entire martensite structure or the entire bainite structure, as shown in Figs. 7a, c. Since the crack will deflect when it passes the M/B phase boundary, the expansion energy for the crack to pass over the phase boundary of the M/B mixed structure increases. This will increase the value of  $K_{lc}$  and reduce the crack's growth rate.

#### V. Conclusion

1. The quenching and tempering structure of high carbon low alloy steel which is pretreated by carbide refining has fine and uniformly distributed carbides. Its crystal grain can be refined to the 11th degree. Comparing with the quenching and tempering structure pretreated by conventional spheroidization, this has higher strength and hardness, and has similar  $K_{lc}$  and ductility. Its pregnant period  $N_o$  of fatigue cracks is much longer. At low  $\Delta K$ , its growth rate of fatigue cracks is low. But as  $\Delta K$  increases,  $da/dN$  increases sharply, and the  $m$  value is high. This heat treatment is mainly used for the enhancement of strength. It is better to apply this treatment to those parts which are operated under low impact loading and high cycle fatigue such that their contact fatigue and wear resistance can be improved.

2. After carbide refining pretreatment, the mixed structure with 50% bainite has higher strength,  $K_{lc}$ , and ductility, and longer pregnant period  $N_o$  of fatigue cracks than those of conventional quenching, tempering and isothermal quenching structures. At higher  $\Delta K$ , it has the lowest growth rate of fatigue cracks.

This treatment is good for the enhancement of strength and toughness and is better applied to those parts which are operated under high  $\Delta K$ .

3. The fracture facet of fatigue cracks shows some characteristics under examination. For high carbon CrWMn steel of cold punch dies with coarse carbide, its fracture is mainly intergranular and has a small amount of microvoid coalescence. For M/B mixed structures after carbide refining, the fatigue fracture is mainly through small dimples with a small amount of quasicleavage. If the percentage of bainite increases to 90%, the fatigue fracture is mainly through quasicleavage. It is obvious that the formation and growth rate of fatigue cracks have a close relationship with the microfracture mechanism.

#### REFERENCES

- [ 1] C. A. Stickels, Met. Trans. 5, 1974, 4, 865
- [ 2] W. Luty, HTM, 32, 1977, 5, 210
- [ 3] Metal Society of Japan, 32, 1968, 12, 1193
- [ 4] L. Huang, Metal Heat Treatment, 1981, 8, 10
- [ 5] R. J. Kan, Met. Trans., 10, 1979, 7, 1711
- [ 6] Yu-Job Song, J. Metal Heat Treatment, 1982, 1, 10
- [ 7] L. Huang, Metal Heat Treatment, 1982, 3, 27
- [ 8] Y. Chen, Metal Heat Treatment, 1982, 9, 51
- [ 9] C. J. Memahon, Acte. Met., 13, 1965, 591
- [10] G. Knass, Met. Trans., V9A, 1978, 1527
- [11] Shou-lin Cheng, Collection of metal strength and fatigue, 1979, 10, 54
- [12] J. Metal Society Japan, 14, 1975, 9, 689
- [13] J. P. Naylor, Met. Trans., 10A, 1979, 7, 861
- [14] Peking Inst. of Electrical Engineering, Industry Dept. of Mechanical Engineering, 1983, 2

**END**

**FILMED**

**3-86**

**DTIC**